Inactivation of genes coding for mitochondrial Nd7 and Nd9 complex I subunits in *Chlamydomonas reinhardtii*. Impact of Complex I loss on respiration and energetic metabolism.

Simon Massoz[a], Véronique Larosa[a], Charlotte Plancke[a], Marie Lapaille[a], Benjamin Bailleul[a], Dorothée Pirotte[a], Michèle Radoux[a], Pierre Leprince[b], Nadine Coosemans[a], René F. Matagne[a], Claire Remacle[a], Pierre Cardol[a*]

Keywords : Chlamydomonas, NADH:ubiquinone oxidoreductase, NAD7/NDUFS2, NAD9/NDUFS3, oxidative stress, energetic metabolism.

[a]Genetics of microorganisms, PhytoSYSTEMS, Department of Life Sciences, [b]GIGA-Neuroscience, University of Liège, Belgium.

Running Title: Impact of complex I loss on energetic metabolism.

*Address correspondence to : Pierre Cardol, Laboratory of Genetics of microorganisms, PhytoSYSTEMS, Department of Life Sciences, University of Liège, B-4000, Liège, Belgium; E-Mail : pierre.cardol@ulg.ac.be; phone : -32-43663840

Abstract

In Chlamydomonas, unlike in flowering plants, genes coding for Nd7 (NAD7/49 kDa) and Nd9 (NAD9/30 kDa) core subunits of mitochondrial respiratory-chain complex I are nucleus-encoded. Both genes possess all the features that facilitate their expression and proper import of the polypeptides in mitochondria. By inactivating their expression by RNA interference or insertional mutagenesis, we show that both subunits are required for complex I assembly and activity. Inactivation of complex I impairs the cell growth rate, reduces the respiratory rate, leads to lower intracellular ROS production and lower expression of ROS scavenging enzymes, and is associated to a diminished capacity to concentrate CO_2 without compromising photosynthetic capacity.

1. Introduction

Rotenone-sensitive NADH:ubiquinone oxidoreductase (Complex I, EC 1.6.5.3) is the largest enzyme complex of the mitochondrial respiratory-chain. This membrane-bound enzymatic assembly of approximately 1000 kDa is composed of 45 subunits in the mammal *Bos taurus* (Carroll et al., 2006), 42 in the fungus *Yarrowia lipolytica* (Angerer et al., 2011), 49 in the land plant *Arabidopsis thaliana* (Peters et al., 2013) and 42 in the green alga *Chlamydomonas reinhardtii* (Cardol et al., 2004). At least 40 subunits are conserved in all eukaryotic lineages (Cardol, 2011). Fourteen of these subunits are homologous to the 14 constituents of the bacterial type-I dehydrogenase and are thus considered as the core of the mitochondrial complex I (Friedrich, 2001). In mammals and fungi, seven hydrophobic subunits (ND1, 2, 3, 4, 4L, 5, and 6) of these 14 components are encoded in the mitochondrial genome and constitute the core of the membrane arm of the complex. Encoded in the nuclear genomes, the 7 remaining subunits (NDUFS7/PSST, NDUFS8/TYKY, NDUFV2/24 kD, NDUFS3/30 kD, NDUFS2/49 kD, NDUFV1/51 kD, NDUFS1/75 kD according to the human/bovine nomenclature) constitute the core of the matricial soluble arm which bears all the prosthetic groups (Fe-S clusters, FMN) that are required for electron transfer from NADH to ubiquinone (Sazanov and Hinchliffe, 2006). Several exceptions to this distribution between mitochondrion-encoded membrane constituents and nucleus-encoded matricial subunits however exist in the green lineage: (i) the mt-DNA of most land plants code for 49 kD (NAD7) and 30 kD (NAD9) hydrophilic subunits; (ii) in the liverwort

Marchantia polymorpha, a *nad7* pseudogene is located in the mtDNA whereas a functional *nad7* gene copy is found in the nuclear genome (Kobayashi et al., 1997); and (iii) the mitochondrial genomes of several chlorophycean unicellular green algae (including *Chlamydomonas reinhardtii* and *Scenedesmus obliquus*) code only for five complex I subunits (ND1, 2, 4, 5 and 6) (Bullerwell and Gray, 2004). Thanks to the sequencing of the nuclear genome of *C. reinhardtii* (Merchant et al., 2007), the *NUO3, NUO7, NUO9,* and *NUO11* algal nuclear genes have been identified as homologs of the ND3, ND7, ND9 and ND4L mitochondrial coding sequences from higher plants (Cardol et al., 2005). To address the question of complex I assembly, *C. reinhardtii* has been demonstrated to constitute a particularly useful experimental model. Complex I-deficient mutants survive in photo-autotrophic conditions (light + mineral medium) due to the operation of rotenone-insensitive alternative NAD(P)H dehydrogenases (Lecler et al., 2012) and because their photosynthetic activity is barely affected (Cardol et al., 2003). Complex I-deficient mutants are also viable in heterotrophic conditions (darkness + acetate as a carbon source). This provides an advantage to screen for complex I mutants, as they display robust growth in the light but slow growth under heterotrophic conditions (Remacle et al., 2008). Several mutations in four of the complex I subunits (ND1, 4, 5, and 6) encoded by the mitochondrial genome have been described so far in Chlamydomonas (Cardol et al., 2008; Cardol et al., 2002; Larosa et al., 2012; Remacle et al., 2001; Remacle et al., 2006). Several complex I-deficient mutants (called *amc* for "**a**ssembly of **m**itochondrial **c**omplex I) of nuclear origin have also been isolated by using a mutagenesis approach (Barbieri et al., 2011). In *C. reinhardtii,* RNA interference is an alternative powerful tool to knock-down the expression of specific nuclear genes (Schroda, 2006). The use of this technique allowed us to determine that ND3 and ND4L subunits are required for complex I activity and assembly in Chlamydomonas (Cardol et al., 2006). RNA interference also allowed us to gain insight into the role of other respiratory chain enzymes, such as F_1F_O ATP synthase (Lapaille et al., 2010), rotenone-insensitive alternative NAD(P)H dehydrogenase (Lecler et al., 2012) and cyanide-insensitive alternative oxidase (AOX) (Mathy et al., 2010).

In this work, we aimed to inactivate the expression of the *NUO7* and *NUO9* nuclear genes (encoding Nd7 and Nd9 subunits) by using the RNA interference or insertional mutagenesis approaches in *C. reinhardtii*. To identify putative alterations of the energetic metabolism in complex I

mutants (as previously observed for AOX–defective mutants of Chlamydomonas (Mathy et al., 2010)), a comparative study of the cellular soluble proteome has been undertaken on a mutant totally deprived of complex I (*dum17* defective in mitochondrion-encoded ND6 subunit).

2. Material and methods

2.1 Strains and culture conditions.

The *C. reinhardtii* strains used in this study are the wild-type 137c (ref. no 1' mt^+ and 2' mt^-) and their derivative *dum17* mt^- (ref no. 233 and 680, bearing a frameshift mutation in mitochondrial *nd6* gene, Cardol et al., 2002), *arg7-8* mt^+ (ref. no 3A+), *arg7-8* mt^- (ref. no 4A-), *cw15* mt^+ (ref. no 25 and 83) and *cw15 arg7-8* mt^+ (ref. no. 325.2) lacking either cell-wall and/or argininosuccinate lyase. Cell cultures were grown in liquid or on agar media under continuous illumination (50 µE. m^{-2}. s^{-1}) at 25°C. The routinely used medium was Tris-minimal-phosphate (TMP) supplemented with 17 mM acetate (TAP) (Gorman and Levine, 1965) . To measure the doubling time of strains, cell numbers were determined with a Z2 Coulter Counter analyzer (Beckman Coulter). Cells were harvested in mid log phase of culture (corresponding to 2-5 x 10^6 cells/ml).

Escherichia coli DH5α was used for cloning gene and cDNA sequences, and *E. coli* transformants were grown in L (Luria) medium in presence of ampicillin (50 µg/ml) or chloramphenicol (10 µg/ml) at 37°C.

2.2 Construction of Plasmids for dsRNA expression.

A summary of DNA constructs for double strand RNA expression in *C. reinhardtii* is shown in Figure 1. Oligonucleotides with restriction enzyme sites were purchased from Eurogentec (Liège, Belgium), T4 DNA ligase and endonucleases from Invitrogen, *Taq* polymerase from Promega. Two plasmids were used to express double strand RNA in *C. reinhardtii*. The pNB1 plasmid (2895 bp) (Cardol et al., 2006) and the pPN10 plasmid (4420 bp) that was obtained by inserting a 1020-bp *Apa*I-*Sal*I fragment of the pPN2 plasmid (Loppes and Radoux, 2001) containing the *NIA1* full promoter into *Apa*I-*Sal*I cohesive ends of the pBCKS+ vector (Stratagene).

2.2.1 Construct of pND9-RNAi plasmid (4189 bp).

A 481-bp fragment of NUO9 cDNA (gb:AY351261) was amplified by PCR with ND9-3F (5'-**ATCGAT**AAGCTTCAGGAGCCCACGATATACACCACG-3') and ND9-4R (5'-AAGCTT**CTGCAG**GCGTCTCCCAAGGGCTGTTG-3') primers containing ***Cla*I**-*Hin*dIII and *Hin*dIII-***PstI*** restriction sites at their 5' ends, respectively. The product was cloned into the pGEM-T easy vector and the excised *Hin*dIII fragment was inserted into the pNB1 plasmid. Constructs with inverse orientation (pND9-AS) were selected by a PCR analysis. The 801-pb corresponding gene fragment containing a 320-bp intron was amplified with the same primers, cloned into the pGEM-T easy vector (pND9-1) and the excised *Cla*I-*Nco*I segment was then inserted into the *Cla*I-*Nco*I sites of pND9-AS to obtain the pND9-RNAi (Figure 1B).

2.2.2 Construct of pND7-RNAi plasmid (6036 bp).

A 719-bp fragment of ND7 cDNA (gb: AY347483) was amplified by PCR with ND7-1F (5'-**GGATCC**AAGCTTGAACAACTTCACGCTGAACTTCGG-3') and ND7-9R (5'-**GAATTC**TGAACTGCATCTTGCCGTACGC-3') primers containing ***Bam*HI**-*Hin*dIII and ***Eco*RI** restriction sites at their 5' ends, respectively. The product was cloned into the pGEM-T easy vector (pND7-2) and the excised *Hin*dIII-*Eco*RI fragment was inserted into the pPN10 plasmid in sense orientation downstream the promoter (pND7-S). A 932-pb cDNA fragment amplified with ND7-1F primer and ND7-8R (5'-**GAATTC**CCTCGGTGTAGAGCTTGAAGTGG-3') primer bearing ***Eco*RI** restriction site at its 5' end, was cloned into the pGEM-T easy vector (pND7-1) and the excised *Bam*HI-*Eco*RI fragment was inserted in inverse orientation into the pND7-S to obtain the pND7-RNAi plasmid (Figure 1A).

2.3 Transformation of *C. reinhardtii* and selection clones.

2.3.1 RNA interference.

Transformation of the *Chlamydomonas cw15 arg7-8 mt*$^{+}$ strain was carried out using the glass-bead method (Kindle, 1990) with 5 µg of pRNAi plasmid (linearized with *Sca*I for pND9-RNAi or *Ssp*I for pND9-RNAi) and 1 µg of pASL, linearized with *Bam*HI. This pASL plasmid bears the *Chlamydomonas ARG7* gene that codes for the argininosuccinate lyase (Debuchy et al., 1989) and is used as a selectable marker. Prototroph transformants were selected on TAP agar plates. The presence

of sequences belonging to the right and to the left part of the RNAi plasmids in the transformants was checked by PCR with primers hybridizing in the *NUO7* or *NUO9* sequences and in the vector (universal primers 5'-GTAAAACGACGGCCAG-3'; 5'-CAGGAAACAGCTATGAC-3'). The stability of the phenotype observed for the transformants mentioned in this study was checked at least one year after their isolation.

2.3.2 Insertional mutagenesis.

Amplification of hygromycin B resistance cassette (HygR, encoded by the *APH7* gene) from the pHyg3 plasmid, electroporation of 3A+ or 4C cells with 100 ng of HygR cassette, and subsequent selection of hygromycine resistant transformants were carried out as described in (Barbieri et al., 2011). The transmission pattern of the dark$^-$ and Hyg^R loci in crosses were determined by random analysis of the meiotic products. Amplification of insertion-linked sequence by thermal asymmetric interlaced (TAIL)-PCR was conducted with degenerate primers as described in (Dent et al., 2005) with *APH7* (hygromycine) specific primers: Hygterm1 (5'-CCGCGAACTGCTCGCCTTCACCT -3'), Hygterm2 (5'-TTCGAGGAGACCCCGCTGGATC-3'), and Hygterm3 (5'-CGATCCGGAGGAACTGGCGCA-3').

2.5 Protein analyses.

Total protein extract or crude membrane fractions were isolated from cells disrupted by sonication (Remacle et al., 2001). Purified mitochondria were obtained according to (Cardol et al., 2002). Proteins amounts were determined by the Bradford method (Bradford, 1976). NADH:ferricyanide oxidoreductase, complex I, complex II+III and complex IV activities were measured according to (Cardol et al., 2002; Remacle et al., 2001). SDS–PAGE was conducted according to standard protocols. Blue Native Polyacrylamide Gel Electrophoresis (BN-PAGE) analyses, and subsequent stainings of the gels by NADH/NBT (nitroblue tetrazolium) or Coomassie blue were performed as previously published (Cardol et al., 2006; Cardol et al., 2004). SDS-gels and BN-gels were electroblotted according to standard protocols. The following antisera raised in rabbits were used: polyclonal antisera raised against whole purified complex I from *Neurospora crassa* (provided by H. Weiss and U. Schulte), Atp2 (β subunit of Atpase) from *Polytomella sp.* (provided by D. González-Halphen; used at a dilution 1:150,000), Aox of *C. reinhardtii* (obtained from S. Merchant;

used at a dilution 1:50,000) or monoclonal antisera raised against PSST (1:2,000) and TYKY (1:2,000) subunits from *Y. lipolytica* (provided by V. Zickermann and U. Brandt). Detection was performed using the BM Chemiluminescence Western blot kit (Roche) with anti-rabbit POD-conjugated antibodies. 2D-DIGE **e**lectrophoresis and protein identification were conducted as previously described (Mathy et al., 2010). Briefly, preparation of each protein extract (25 µg) and labeling with CyDye (GE Healthcare) were conducted in triplicate. 3-11 NL IPG Drystrips (GE Healthcare) were used and images of 2D gels were analyzed with the DeCyder 6.5 software (G. E. Healthcare). For protein identification, preparative gels were loaded with 750 µg protein and spots of interest were picked using an Ettan Dalt Spot Picker (GE Healthcare). Proteins were subsequently digested in-gel and the resulting peptides mixtures were analyzed in MS and in LIFT MS/MS modes (Ultraflex II MALDI TOF TOF, Bruker Daltonic, Laboratory of mass spectrometry, GIGA, University of Liège, Belgium). Protein identification was carried out using the Mascot search engine. Mass error was fixed at 70 ppm and peptide modifications were assessed as cysteine carbamidomethylation (fixed modification) and methionine oxidation (as a variable modification).

2.6 RNA analyses.

Total RNA was extracted as previously described (Loppes and Radoux, 2001). For RNA blot analyses, RNA (15 µg) was separated on 0.8 % agarose/formaldehyde gels and transferred onto Hybond N+-membrane (Amersham Pharmacia Biotech). Dig-labelled PCR products of cDNA fragments were used as gene probes and detected with anti-DIG-AP-conjugates and CDP-Star as substrate (Roche). Probes for detection of *NUO3, NUO7 NUO9, NUO11, NUO17,* and *NUOP1* were obtained as previously described (Cardol et al., 2006)

2.7 *In vivo* analysis of photosynthesis and respiration.

Respiratory and photosynthetic activities were measured as O_2 exchanges rates using a Clark-type oxygen electrode at 25°C (Hansatech Instrument, King's Lynn, England). Saturation of photosynthesis was achieved at ~1000 µmol photons at 640nm . m^{-2} . s^{-1}. PSII antenna size was evaluated by measuring the rate of chlorophyll fluorescence induction (half-time, $t_{1/2}$, s) from open (F_O) to closed (Fm) PSII centers in the presence of 3-(3,4-dichlorophenyl)-1,1-dimethylurea (DCMU) at low light (<200 µmol photons at 630 nm . m^{-2} . s^{-1}) with a JTS-10 spectrofluorometer (Biologic,

France). This parameter is quantitatively related to the absorption cross-section of PSII (Butler, 1978). Hydrogen peroxide levels were determined by staining with 3-3' diaminobenzidine (DAB) (Sigma) as described previously (Mathy et al., 2010). Filters with cell deposits were incubated during 20 min at 50 µE. m^{-2}. s^{-1}.

2.8 *In silico* analyses.

Frequency of codon utilization was compared with data available for *C. reinhardtii* nuclear genes (http://www.kazusa.or.jp/codon/). Peptide signal was predicted using the Predalgo program (https://giavap-genomes.ibpc.fr/cgi-bin/predalgodb.perl?page=main) (Tardif et al., 2012). Alpha-helix predictions were computed with the Deleage-Roux and Levitt scales with the Protscale program on the Expasy server (http://us.expasy.org/). Position of residues along alpha helixes (3.6 residues per turn) was determined with the Pepwheel program (http://emboss.bioinformatics.nl/cgi-bin/emboss/pepwheel) (Ramachandran and Sasisekharan, 1968).

3. Results

3.1 *NUO7* and *NUO9* genes possess features of Chlamydomonas nuclear genes and their polypeptide products are adapted for import into mitochondria.

The endosymbiotic event that gave rise to mitochondria was followed by a massive migration of genes from the endosymbiont to the nucleus (Gray et al., 1999). As well as the highly hydrophobic components of complex I, the hydrophilic NAD7 and NAD9 subunits from most flowering plants remain encoded in the mitochondrial genome. In contrast, these genes are missing from the mitochondrial genome of *C. reinhardtii*, as it is also the case in mammals and fungi. We previously identified the *NUO7* and *NUO9* nuclear genes of *C. reinhardtii* (encoding Nd7 and Nd9 subunits) as homologs of the sequences encoding flowering plant NAD7 and NAD9 subunits, respectively (Cardol et al., 2004). To be efficiently expressed, mitochondrial genes that have been transferred to the nucleus have to acquire several distinct traits typical of nuclear genes and absent in mitochondrial genes (González-Halphen et al., 2004). (i) *Efficient promoter*. Based on signals obtained on Northern blot experiments (as shown in Figure 2), one can infer that both *NUO7* and *NUO9* genes have acquired

efficient promoters. (ii) *Changes in codon usage.* The pattern of codon usage in *NUO7* and *NUO9* genes is typical of nuclear genes (Table S1). Moreover, the GC content of both genes is about 63% and fits well with that of the nuclear genome (64%) (Merchant et al., 2007). In contrast, the GC content is only 45 % for mtDNA (GenBank U03843 accession number). (iii) *Acquisition of polyadenylation signal.* The polyadenylation signal of *C. reinhardtii* nuclear genes (TGTAA) (Silflow, 1998) is found at the end of cDNA sequences (GenBank XM_001697555 and XM_001690600 accession numbers). (iv) *Acquisition of introns.* Intronic sequences with orthodox splicing sites (Silflow, 1998) were identified: eleven were found in the *NUO7* gene (Phytozome Cre09.g405850 accession number) and one in the *NUO9* gene (Phytozome Cre07.g327400 accession number). (v) *Presence of a putative mitochondrial targeting sequence (MTS).* Most nucleus-encoded mitochondrial proteins contain a targeting sequence that sorts the intracellular localization (Glaser et al., 1998). When the deduced full-length ND7 and ND9 sequences were compared to the polypeptidic sequences of flowering plants, N-terminal extensions of about 75 and 85 residues, respectively, were found (Figure S1). A targeting prediction to mitochondria was also given by Predalgo program (Tardif et al., 2012), with a peptide signal of 57 and 71 amino acids which possess all characteristics of MTS : (a) their composition is similar to the composition described for MTS of higher plants (Glaser et al., 1998) (data not shown); (b) the N-terminal residues (1 to 18) have the potential to form amphiphilic α helixes with one hydrophilic and positively charged face and one apolar face (Figure 1D). This amphiphilicity seems to be essential for the function of MTS (Emanuelsson et al., 2000). (c) Putative cleavage sites (Glaser et al., 1998) are found after residue 70 (RS↓AT) for Nd7 and residue 73 (RX_7RK↓TT) for Nd9, which is consistent with the length of their protein homologues encoded by mtDNA from plants. Moreover, the deduced molecular masses of mature Nd7 (45211 Da) and Nd9 (24462 Da) subunits are in good agreement with their identification in SDS gel by mass spectrometry as 43 and 25-kDa bands of complex I, respectively (Cardol et al., 2004).

3.2 RNAi mutants defective in *NUO7* or *NUO9* gene expression lack complex I activity.

To suppress the expression of *NUO7* and *NUO9* genes (coding for Nd7 and Nd9 complex I subunits, respectively), a cell-wall less strain of *C. reinhardtii* auxotroph for arginine (strain 325.2)

was co-transformed with the pASL plasmid (bearing the *ARG7* gene), and the plasmid designed for RNA interference (pND7-RNAi or pND9-RNAi, Figure 1). One hundred and twenty arg^+ colonies of each transformation experiment were selected and tested by PCR for the presence of a pRNAi plasmid partial sequence in their genome, as described in point 2.3.1. Thirteen and seventeen co-transformants, called coND7 and coND9 clones, respectively, were obtained.

To investigate complex I activity in the cotransformants, high molecular-mass complexes from crude membrane fractions were separated by BN-PAGE. NADH dehydrogenase activity of the complex I matricial arm was then tested using NBT as an electron acceptor. Wild-type complex I activity was associated with a single band at 950 kDa, as previously found (Cardol et al., 2002; Cardol et al., 2004). The staining level of each clone was determined and reported as a percentage of the wild-type staining. One coND7 clone (19) and two coND9 clones (54 and 115) showed a very low activity (~5%) after two hours of incubation in the staining reaction mixture.

To determine whether the complex I activity defect detected in coND7-19 mutant was correlated to a specific degradation of *NUO7* transcripts, the transcription levels of *NUO3*, *NUO7*, *NUO9*, *NUO11*, *NUO17* and *NUOP1* genes, coding for ND3, ND7, ND9, ND4L, ESSS/NDUFB11 and B14.5b/NDUFC2 complex I subunits (bovine/human nomenclature), were investigated by Northern blot analyses (Figure 2A). *NUO7* transcripts was almost absent in coND7-19 whereas the levels of other transcripts were similar to the control strain. A similar analysis showed that *NUO9* transcript was undetectable in coND9-54 and coND9-115 mutant strains, while other transcript amounts (*e.g. NUO11*) were equivalent to those detected in wild-type cells (Figure 2B). Taken together, these results indicates that the complex I activity defect detected in the mutants is due to a specific loss of the *NUO7* or *NUO9* transcripts triggered by the RNA interference machinery.

The frequency of transformants showing an altered complex I defect among those bearing the inactivation cassette was thus about 10%. This frequency is similar to the one reported in previous studies dedicated to the inactivation of other genes in other cellular processes by RNAi approach in Chlamydomonas (Schroda, 2006).

Complex I-defective mutants show slow growth when cultivated under heterotrophic conditions (see Introduction). In the light, they also show a reduced growth compared to wild-type

cells when fed with an exogenous organic carbon source (*e.g.* acetate) (Cardol et al., 2002; Remacle et al., 2001). In the light without acetate (phototrophic growth), the doubling time determined for wild-type cells (83h ± 11h) did not differ significantly from the values obtained for mutant cells, meaning that when the cell metabolism relies mainly on photosynthesis (*i.e.* phototrophic growth), complex I activity plays a minor role in cell energetic. The difference between wild type and complex I mutants was however more pronounced when the mitochondrial metabolism was stimulated by acetate in the light (mixotrophic growth). For wild-type wall-less cells, the doubling time obtained (13h ± 3 h) was in good agreement with previous reports (Baroli et al., 2004), while it was ~ 1.5 higher for mutants (19h ± 3h for coND7-19, 21 ± 3 for coND9-54 and -115). Therefore, all experiments were conducted on cells grown in the presence of acetate in the light.

Respiration of complex I mutant also lacks sensitivity to rotenone (Remacle et al., 2008), a potent inhibitor of ubiquinone reduction in complex I. Dark respiration rate of mutants grown in mixotrophic conditions were found to be ~40 % inferior to the value obtained for wild-type cells (about 40 nmoles O_2 . min^{-1} per 10^7 cells) and almost insensitive to rotenone (Table 1).

3.3 An insertion in the promoter region of *NUO9* gene partly impairs complex I activity in *amc14* mutant.

A previous forward genetic screen allowed to isolate seven *amc* nuclear mutants (for **a**ssembly of **m**itochondrial **c**omplex I) displaying reduced or no complex I activity (Barbieri et al., 2011). To uncover additional AMC loci, we undertook another screen for nuclear mutants defective in complex I (see 2.3.2). Out of ~3000 insertional hygromycine-resistant transformants, 5 showed features of complex I-defective mutants. One mutant strain (further named *amc14*) showed a reduced growth in heterotrophic (darkness + acetate) and mixotrophic (light + acetate) conditions (Figure S2A). Its rotenone-sensitive respiration was about 40% of the control wild-type strain. Moreover, in-gel staining of NADH dehydrogenase activities indicated that ~ 30-50 % complex I activity was retained (Figure S2B). Since the antibiotic resistance cosegregated with the *amc* phenotype (data not shown), we concluded that the AMC14 locus was tagged with the insertional marker. Using TAIL-PCR mapping, we found that the insertional marker was located in the promoter region of the *NUO9* gene, 132 bp upstream of the initiation codon (Figure 1C and S2C). The size of the deletion that

accompanied the insertion of the marker was at most 31 bp. Figure 2C shows that the amount of *NUO9* transcript was greatly reduced in *amc14*. We can thus conclude that the insertion in the promoter region of *NUO9* gene impairs expression of the corresponding transcript.

3.4 Lack of complex I activity and assembly in the absence of Nd7 or Nd9 subunits.

To confirm the defect in complex I activity due to impairment in *NUO7* or *NUO9* gene expression, enzyme activities were measured in crude membrane fractions and compared to values obtained for wild type (Table 1). In the RNAi mutants, the NADH:duroquinone oxidoreductase activity sensitive to rotenone (considered to represent the activity of complex I) was found to be null or almost null and the NADH:ferricyanide oxidoreductase which is mainly catalyzed (70-85%) by the matricial arm of complex I in Chlamydomonas (Cardol et al., 2002) was about 15-30 % of wild-type activity. These results are similar to those obtained for mitochondrial *dum17* mutant defective in complex I ND6 subunit (Table 1). In the *amc14* mutant, the complex I and NADH:ferricyanide oxidoreductase activities were however up to 50-60% of the wild-type values. These results agree with the complex I defect observed by in-gel staining activities (Figure S2B) and reduced amount of *NUO9* transcript. In contrast, cytochrome *c* oxidase activity was determined as control and no significant difference could be observed between wild-type and mutant strains.

In order to gain further insights into the impact of the loss of Nd7 or Nd9 on membrane complex assembly, whole membrane fractions from RNAi complex I- null mutants and wild type were purified and subjected to BN-PAGE analyses. By staining the gel with Coomassie blue, respiratory-chain dimeric complex V (1600 kDa, Villavicencio-Queijeiro et al., 2009) and complex I (950 kDa Cardol et al., 2004) were detected in wild-type extract (Figure 3A). In contrast, no complex I was observed in the RNAi mutants while the amount of dimeric complex V was not altered. These results were confirmed by comparing the amount of three proteins in membrane fraction by immunodetection on Western blot after SDS-PAGE : TYKY (complex I subunit encoded by *NUO8* gene), β subunit (complex V subunit encoded by *ATP2* gene) and Aox (respiratory-chain alternative oxidase) (Figure 3D) . In order to identify putative complex I subcomplexes, the protein complexes separated by BN-PAGE were also tested by immunodetection on Western blots with antisera against whole *N. crassa* complex I or against subunit PSST of *Y. lipolytica* (homologous of *C. reinhardtii* complex I subunit

encoded by *NUO10* gene). In wild type, only the whole complex I is highlighted by both antibodies whereas no signal could be detected for mutants (Figure 3B,C).

3.5 The loss of complex I leads to slight modifications in the energetic metabolism.

We previously showed that among respiratory-deficient mutants, those affected solely for complex I activity were the less affected regarding their ATP content and photosynthetic electron transfer chain in the chloroplast (Cardol et al., 2003). In order to analyze the main consequences of suppression of complex I activity on the metabolic network of the cell, we carried out a comparative study on the cellular soluble proteome. This analysis was performed by using the mitochondrial *dum17* mutant which is fully defective in complex I and possesses a cell-wall (knock-out strain, mutated in the mitochondrial encoded *nd6* gene (Cardol et al., 2002)), instead of cell-wall less RNAi strains that are knock-down strains. To minimize variations between strains due to genetic drift, we compared two *dum17* mutant strains isolated 10 years ago (233 and 680 strains in our stock collection) with two wild-type strains (1' and 2' strains in our stock collection). A total of ~4800 protein spots were detected on the 2D gels (Figure S3, pH range 3-11 non linear). Based on a statistically significant Student's t-test ($p < 0.05$, $n=3$) for higher than 1.3-fold increase or lower than 1.3-fold decrease in ratio of normalized spot abundance for 3 comparisons out of 4 (233/1', 233/2', 680/1', 680/2'), 58 protein spots were accepted as being differentially expressed between wild-type and *dum17* mutant strains. Sixteen of them were identified along with 140 protein spots displaying no variation (Table 3 and Table S2). Only proteins related to energetic metabolism, which constituted the majority of identified spots, have been considered in the following analysis.

Apart from two complex I subunits that show a strong decrease in their expression, proteins belonging to respiratory-chain complex III and ATP synthase did not show any modification, confirming that the lack of complex I has no impact on the major constituents of the respiratory chain (Cardol et al., 2008; Cardol et al., 2002; Remacle et al., 2001). Several proteins involved in Krebs cycle, glyoxylate cycle or glycolysis were also identified and none varied, at the exception of one spot over seven corresponding to aconitate hydratase. In contrast, we observed an increase of the amount of two aspartate amino acid transferases (Ast1, Ast3) and we found a down-regulation of three major ROS scavenging enzymes, namely mitochondrial Mn superoxide dismutase (Msd1, -1.7), chloroplastic

Fe superoxide dismutase (Fsd1, -1.5) and cytosolic glutathione S-transferase (GstS2, -1.6). Since superoxide dismutases are scavengers of O_2^- into H_2O_2, we tested peroxide production. In *dum17* complex I-deficient cells, it was 35% inferior to the amount measured in wild type. Although not significant, a decrease was also observed in RNAi mutants (Table 2).

Regarding photosynthesis, two spots corresponding to components of PSII light-harvesting complex (Lhcbm2 and Lhcb5/CP26) showed a significant decrease (-1.5) but no differences were observed between wild type and complex I-deficient mutants either for spots corresponding to other Lhc proteins (identified as Lhcbm1, 2, 3,10) or for PSII absorption cross section by fluorescence measurements (Table 2). A decrease in the amount of the carbonic anhydrase (alpha-type Cah1) located in the periplasm was observed and one spot corresponding to small subunit of Rubisco (RbcS) also showed a very strong decrease (-3.7) even when this was not paralleled with a reduced amount of the large subunit (RbcL) (13 identified spots) or with a difference in Rubisco amount on native gels (Figure 3). To determine whether photosynthetic capacity could be modified in the complex I-deficient mutants, polarographic measurements of oxygen exchange rates were performed. The maximum rates of oxygen evolution at saturating light intensity (>1000 µE. m^{-2}. s^{-1}) did not differ between wild type, *dum17* and RNAi mutants (Table 2). Supporting these results, numerous other chloroplastic proteins involved in photosystem II, light harvesting complex (including one additional spot corresponding to Lchbm2), pentose phosphate pathway or chlorophyll biosynthesis, have been identified and none did significantly vary between wild type and complex I mutant. The abundance of PSI and PSII complexes in association with Lhc complexes in wild-type and mutant cells has also been estimated on BN-gels (Figure 3A) and no difference could be observed. Additionally, spectrophotometric measurements of total chlorophyll (Chl_{a+b}) content in methanolic extract indicated that there is no significant difference between wild-type and mutants cells (Table 2).

4. Discussion

Nd7 and Nd9 are two components of mitochondrial complex I in *C. reinhardtii* (Cardol et al., 2004). Belonging to the matricial arm of the complex, they are homologous to plant mitochondria-encoded NAD7 and NAD9, human nucleus-encoded 49kD/NDUFS2 30 kD/NDUFS3 subunits and

NuoD/C subunits of bacterial NDH-1 complex. In this work, we report the inactivation of the corresponding nuclear genes (*NUO7* and *NUO9*) in Chlamydomonas. Despite the fact that the two proteins are the only core subunits of the matricial arm that do not provide ligands for cofactors (FMN and Fe-S clusters) (Hinchliffe and Sazanov, 2005), their loss leads to the absence of complex I in Chlamydomonas, as also observed in all species investigated so far. In the fungus *N. crassa,* the disruption of the corresponding genes prevents the activity and assembly of the matricial arm while a membrane part of the complex is still present in mitochondrial membranes (Duarte et al., 1998; Schulte and Weiss, 1995). In *E. coli*, the nuoC gene encodes a fused version of the two subunits (Braun et al., 1998). Although no structurally intact complex is present in membranes of the nuoC-null mutant, a soluble 170 kD fragment corresponding to the NADH dehydrogenase module (NuoE/NDUFV2/24 kD, NuoF/NDUFV1/51 kD, NuoG/NDUFS1/75 kD) is still active (Erhardt et al., 2012). In tobacco (*Nicotiana sylvestris*), CMSI/II mutants are impaired in the expression of chloroplastic nad7 gene (Lelandais et al., 1998; Pla et al., 1995). As a consequence, rotenone-sensitive oxygen uptake is decreased and there is no complex I assembly (Gutierres et al., 1997; Pineau et al., 2005). The Chlamydomonas *amc14* mutant isolated in this work bears an insertion in the promoter region of *NUO9* gene, which consequently reduces gene expression and lowers in parallel complex I activity and assembly (data not shown), suggesting that the amount of fully assembled complex I is at least controlled by the amount of Nd9 subunit. In mutants deprived of ND1,3-6,or 4L membrane component, we reported the presence of a soluble ~200 kDa fragment showing NADH dehydrogenase activity which was attributed the a fraction of the matricial arm corresponding to the NADH dehydrogenase module (Cardol et al., 2006; Cardol et al., 2002). In human, the NADH dehydrogenase module (comprising notably NDUFV2/24 kD, NDUFV1/51 kD and NDUFS1/75 kD) is distinct from the hydrogenase module (comprising notably NDUFS3/Nd9, NDUFS2/Nd7, NDUFS7/PSTT, NDUFS8/TYKY) and these two fractions (fractions FP and IP, respectively, e.g. Sazanov et al., 2000) are assembled separately (Antonicka et al., 2003; Vogel et al., 2007). In *NUO7* and *NUO9* knock-down Chlamydomonas mutants, while we found the soluble ~200 kD NADH dehydrogenase activity along with the 75 kD (NDUFS1) subunit detected in membrane extract (data not shown), subunits NDUFS7/PSTT, NDUFS8/TYKY of the hydrogenase module are absent. Interestingly it has been

shown in human cell lines that two chaperones (NDUFAF3 and NDUFAF4) cooperate from early to late stages of complex I assembly in association with at least NDUFS3/Nd9, NDUFS2/Nd7, NDUFS8/TYKY (i.e. the hydrogenase module, Saada et al., 2009). Since most chaperones (including NDUFAF3 and NDUFAF4) and core subunits identified in human are conserved in Chlamydomonas (Cardol, 2011; Remacle et al., 2012), this strongly reinforces the idea that the assembly steps of complex I are conserved between human and Chlamydomonas (Cardol et al., 2008; Remacle et al., 2008).

Complex I is acknowledged as a main contributor to superoxide production by mitochondria, where O_2 reacts with reduced flavin mononucleotide (Esterhazy et al., 2008; Kussmaul and Hirst, 2006). ROS (reactive oxygen species) are considered to be a major cause of cellular oxidative stress. In Chlamydomonas complex I mutant, concomitantly to a lower amount of mitochondrial Msd1, chloroplastic Fsd1 superoxide dismutase, and glutathione S-transferase Gst1, the H_2O_2 content was also lowered. Altogether, these observations suggest that in Chlamydomonas, the lower respiratory rate associated to complex I loss limits superoxide production and triggers the down regulation of ROS-scavenging enzymes.

Another notable difference in protein expression between complex I-deficient mutant and wild type is the strong down regulation of the periplasmic alpha carbonic anhydrase (Cah1). Carbonic anhydrase is the usual marker for Chlamydomonas cells grown under CO_2-limiting conditions (Miura et al., 2004). Transcript abundance of *CAH1* and activity of Cah1 were also considerably reduced by the addition of 10 mM acetate without compromising the photosynthetic capacity. This reduction could result from an increased internal CO_2 concentration generated by high, acetate-stimulated respiratory rates (Fett and Coleman, 1994). The level of *CAH1* transcript also decreases in cells subjected to ROS (oxygen peroxide, singlet oxygen, etc), which led the authors to propose the existence of a cross talk between oxidative stress and regulation of the carbon-concentrating mechanism (Ledford et al., 2007). In this regard, the downregulation of Cah1 in complex I mutants also does not impair photosynthetic capacity and is not related to the lowering of ROS production observed in mutant cells. It might result from an increase of the internal CO_2 related to a lower CO_2 demand of cells (lower generation time) whatever is the rate of acetate assimilation.

In complex I-deficient mutants, only the respiratory complexes III and IV still contribute to the formation of the proton electrochemical potential and thus to the production of ATP (Cardol et al., 2003), which accounts for the "slow" growth phenotype of the mutants in the dark. Lower capacity of complex I-deficient mutant cells to reoxidize cellular NADH must limit the rate of catabolic pathways (Krebs cycle, glycolysis and acetate assimilation). In photosynthetic organisms, reducing equivalents generated by photosynthetic electron transfer chain can in part be consumed by the mitochondrial respiratory chain, owing to metabolic exchanges between the two organelles (reviewed in Cardol et al., 2011; Noctor et al., 2007). This process can be mediated by the activity of the malate-aspartate shuttle (Noguchi and Yoshida, 2008), whose genes are present in Chlamydomonas (Merchant et al., 2007). Four enzymes participate in the malate shuttle: two membrane antiporters (glutamate/aspartate and malate/α-ketoglutarate) and soluble enzymes located at both sides of the mitochondrial and chloroplastic membranes (malate dehydrogenase, and aspartate aminotransferase). Aspartate aminotransferase (AAT), also called aspartate transaminase (AST), catalyzes the reversible conversion of aspartate and α-ketoglutarate to oxaloacetate and glutamate. Both the mitochondrial (Ast1) and chloroplastic (Ast3) AAT are upregulated in response to complex I deficiency supporting the idea that the import/export of reducing equivalents is critical for cell bioenergetics.

In mixotrophic conditions, when compared to wild type, complex I mutants of Chlamydomonas are slightly more towards state II transition of the photosynthetic apparatus (Cardol et al., 2003), a condition in which plastoquinones are reduced by the activity of the NAD(P)H dehydrogenase Nda2 (Jans et al., 2008), LHCII are phosphorylated and associated to PSI (reviewed in Lemeille and Rochaix, 2010). In complex I-deficient cells, we found that two protein spots corresponding to LHCII proteins Lhcb5/CP26 and Lhcbm2 were less abundant than in wild type but this was not paralleled with a change in other LHCII protein amounts, PSII-LHCII amount, or PSII absorption cross section. Both proteins play a critical role in state transition process and Lhcb5/CP26 is phosphorylated upon state transition (Ferrante et al., 2012; Takahashi et al., 2006). This might indicate that the decrease in Lhcb5 protein observed in complex I mutant is due a slight difference in the ratio between non-phosphorylated/phosphorylated Lhcb5/CP26 protein. The photosynthetic characterization of Chlamydomonas mitochondrial mutants has highlighted a significant role for the

metabolic interactions between the chloroplast and the mitochondrion. Up to a 75% decrease of the photosynthesis efficiency was found in the case of *dum19*/*25*, a double mutant lacking the respiratory complexes I and IV activities whereas this parameter was barely affected in complex I mutants (Cardol et al., 2003).

As a general conclusion, we can say that despite the halving of respiration rate and growth rate observed in mutant cells compared to wild type when cultivated in mixotrophic conditions, complex I mutants do not show major modifications in the expression of metabolic pathways. As a direct comparison, in a mutant deprived of the alternative oxidase (Aox1) of the respiratory chain, although total respiration and growth were not impaired in mixotrophic conditions, a strong increase of intracellular ROS content was observed. By the same comparative proteomic approach, major modifications in the expression of proteins of primary metabolism were described in Aox1 mutant, namely a decrease of enzymes of the main catabolic pathways, an increase of enzymes involved in anabolic pathways and a strong up-regulation of the ROS scavenging systems enzyme (Mathy et al., 2010). This suggests that the sensing of oxidative stress in the mitochondria would be a primary event that leads to the genetic control of the general metabolic pathways.

Acknowledgments. We thank JH Schumacher, B. Horrion and S. Borenzstein for technical help. This work was supported by a FP7-funded project (Sunbiopath, GA245070), University of Liège (SFRD-11/05), the Fonds National de la Recherche Scientifique (an Incentive Grant for Scientific Research MIS F.4520, FRFC 2.4597.11; FRFC 2.4567.11; CDR J.0138.13) and an FRSM grant (3.4559.11 to PL). VL is a Postdoctoral Researcher, PL and PC are Research Associate of F.R.S.-FNRS.

Figure Legends

Figure 1. A-B, Schematic representation of double-strand (ds)RNAi constructs. *Xba*I/*Hind*III fragments of pND7-RNAi (A), and pND9-RNAi (B). PNIA1 : promoter of the Chlamydomonas *NIA1* gene encoding nitrate reductase. PNIA1/TUB1 : 229-bp chimeric promoter. Numbers within rectangles correspond to the selected exons of the *NUO7* and *NUO9* genes (i = intron). For *NUO9*, we cloned an intron-containing gene fragment, directly linked to its cDNA antisense counterpart, downstream a chimeric promoter composed of 84-bp sequence of the *NIA1* promoter fused to a minimal β-tubulin promoter. For *NUO7*, we cloned two complementary cDNAs fragments in opposite orientation downstream the complete *NIA1* promoter. **C**, Schematic representation of *NUO9* gene with localization of the insertion in *amc14*. Numbers refers to bases relative to the initiation site of translation. **D**, Position of the 18 N-terminal residues of ND7 and ND9 polypeptides along α helixes. Positively-charges residues are marked by a +. Non-polar residues are squared. Predicted apolar face of the amphiphilic helix is shaded.

Figure 2. Transcriptional analysis of several complex I genes in coND7 (A), coND9 (B), and *amc14* (C) mutant strains. Hybridization patterns were obtained with *NUO3*, *NUO7*, *NUO9*, *NUO11*, *NUO17*, and *NUOP1* probes on RNA blot (see methods for details). An approximate size (in kb) is given for each transcript.

Figure 3. Analysis of mitochondrial and chloroplastic native complexes in coND7 and coND9 mutants. 120 µg of crude membrane proteins were loaded on a BN-gel. After electrophoresis, the gel was submitted to NADH/NBT staining (*, NADH/NBT staining) and further stained with Coomassie blue (A) or blotted and probed with antisera against the whole complex I (B) or against PSST subunit (C). I and V_2 correspond to respiratory-chain complexes I and V (dimeric state), respectively. Based on their electrophoretic mobility (Rexroth et al., 2004), PSI and PSII were identified. PSI, PSII, LHCI, LHCII correspond to photosynthetic complexes I, II, and to Light harvesting complexes I, II. (D) 25 µg of crude membrane proteins were subjected to SDS-PAGE, blotted and probed with antisera against TYKY, ATP2 and AOX proteins.

Figure S1. Sequence alignments of the *NUO9* (A) and *NUO7* (B) homologous genes obtained using the MUSCLE (http://www.ebi.ac.uk/Tools/msa/muscle/) and BOXSHADE (http://www.ch.embnet.org/software/BOX_form.html) programs.

(A) Nc , *Neuropsora crassa* (GI:85086366); Rc , *Rhodobacter capsulatus* (GI:294677056); Mm , *Mus musculus* (GI:58037117). Hs , *Homo sapiens* (GI:4758788). Bt , *Bos taurus* (GI:128860); Cr , *Chlamydomonas reinhardtii* (GI:159464845). Pw , *Prototheca wickerhamii*(GI:11497471). No , *Nephroselmis olivacea* (GI:110225659); Mp , *Marchantia polymorpha* (GI:11467145); St , *Solanum tuberosum* (GI:38605724); Ta , *Triticium aestivum* (GI:81176530) .

(B) Nc (GI:164427900); Rc (GI:294677057); Mm (GI:148707168). Hs (GI:4758786). Bt (GI:115495721); Cr (GI:159479042). Pw (GI:11497462) ; No (GI:110225668); Mp (GI:11466758); St (GI:108773185); Ta (GI:81176545).

Identical and similar residues are colored in red and blue, respectively. Yellow color is the position of the amphiphilic alpha helixes as shown in Figure 1D. Underlined sequence is the peptide signal according to predalgo Website (https://giavap-genomes.ibpc.fr/cgi-bin/predalgodb.perl?page=main). Putative cleavage sites of N-terminal presequences are indicated in green/red shaded letters.

Figure S2. A. Growth Phenotype of wild-type and *amc14* strains after 5 days of mixotrophic growth (50 µE . m^{-2} . s^{-1}) on TAP medium (left panel) or after 10 days of heterotrophic growth on TAP medium (right panel). Before plating, cell suspension was normalized ($A_{750\ nm}$ = 0.2). **B.** Complex I activity shown on Blue-Native Gel of proteins solubilized by addition of Triton X-100 (2%) on crude membrane extracts from wild type, *amc14* and coND9-54 mutants. Each lane was loaded with 110µg proteins. The BN-gel was stained for NADH dehydrogenase activity using NBT as an electron acceptor. The colored band at ~950kDa corresponds to respiratory-chain complex I. The lower green band corresponds to a photosynthetic complexe. **C**. (i) Localization of the insertion in *amc14*. Picture illustrating the position of primers used in PCR experiments to estimate the localisation of the insertion in the *amc14* mutant strain; (ii) PCR experiment aiming to amplify the region surrounding the insertion area (264 bp in WT with primers NUO9-F GAACAGGTGCGAGCTTAC and NUO9-R TCATCGTGCGACAGAAGC); (iii) PCR experiment aiming to check the integrity of the genomic

NUO9 sequence corresponding to the transcript (1909 bp with primers NUO9-1R : GCGGACATACGACACTTC and NUO9-5F : CACTGCGTTGCATTGCTTG). GeneRuler TM 1kb plus DNA ladder was used as marker.

Figure S3. Comparison of representative 2D-gel images of (A) WT (1') and *dum17* mutant (233) and (B) WT (1') and *dum17* (680) mutant. Identification number and CyDye used are indicated on top left corner of each gel image. The contour and name of identified proteins that show a significant difference in abundance as listed in Table 3 or Table S2 are indicated. Note the striking difference in intensity of the carbonic anhydrase spots at the center of the images. For each image acidic and basic sides are on the left and right respectively. Low MW proteins migrate to the bottom of the gels.

Bibliographic list

Angerer, H., Zwicker, K., Wumaier, Z., Sokolova, L., Heide, H., Steger, M., Kaiser, S., Nubel, E., Brutschy, B., Radermacher, M., Brandt, U., Zickermann, V., 2011. A scaffold of accessory subunits links the peripheral arm and the distal proton pumping module of mitochondrial complex I. Biochem J 437, 279-288.

Antonicka, H., Ogilvie, I., Taivassalo, T., Anitori, R.P., Haller, R.G., Vissing, J., Kennaway, N.G., Shoubridge, E.A., 2003. Identification and characterization of a common set of complex I assembly intermediates in mitochondria from patients with complex I deficiency. J. Biol. Chem. 278, 43081-43088.

Barbieri, M.R., Larosa, V., Nouet, C., Subrahmanian, N., Remacle, C., Hamel, P.P., 2011. A forward genetic screen identifies mutants deficient for mitochondrial complex I assembly in Chlamydomonas reinhardtii. Genetics 188, 349-358.

Baroli, I., Gutman, B.L., Ledford, H.K., Shin, J.W., Chin, B.L., Havaux, M., Niyogi, K.K., 2004. Photo-oxidative stress in a xanthophyll-deficient mutant of Chlamydomonas. J Biol Chem 279, 6337-6344.

Bradford, M.M., 1976. A rapid and sensitive method for the quantitation of microgram quantities of protein utilizing the principle of protein-dye binding. Anal. Biochem. 72, 248-254.

Braun, M., Bungert, S., Friedrich, T., 1998. Characterization of the overproduced NADH dehydrogenase fragment of the NADH:ubiquinone oxidoreductase (complex I) from Escherichia coli. Biochemistry 37, 1861-1867.

Bullerwell, C.E., Gray, M.W., 2004. Evolution of the mitochondrial genome: protist connections to animals, fungi and plants. Curr. Opin. Microbiol. 7, 528-534.

Butler, W.L., 1978. Energy distribution in the photochemical apparatus of photosynthesis. Ann. rev. Plant Physiol. 29, 345-378.

Cardol, P., 2011. Mitochondrial NADH:ubiquinone oxidoreductase (complex I) in eukaryotes: A highly conserved subunit composition highlighted by mining of protein databases. Biochim Biophys Acta 1807, 1390-1397.
Cardol, P., Boutaffala, L., Memmi, S., Devreese, B., Matagne, R.F., Remacle, C., 2008. In Chlamydomonas, the loss of ND5 subunit prevents the assembly of whole mitochondrial complex I and leads to the formation of a low abundant 700 kDa subcomplex. Biochim Biophys Acta 1777, 388-396.
Cardol, P., Forti, G., Finazzi, G., 2011. Regulation of electron transport in microalgae. Biochim Biophys Acta 1807, 912-918.
Cardol, P., Gloire, G., Havaux, M., Remacle, C., Matagne, R., Franck, F., 2003. Photosynthesis and state transitions in mitochondrial mutants of Chlamydomonas reinhardtii affected in respiration. Plant Physiol. 133, 2010-2020.
Cardol, P., González-Halphen, D., Matagne, R.F., Remacle, C., 2005. Update on the mitochondrial OXPHOS proteome of the green alga *Chlamydomonas reinhardtii*, in: végétale, S.F.d.B. (Ed.), 7th International Congress on plant mitochondrial biology (ICPM), Obernai, France, p. P18.
Cardol, P., Lapaille, M., Minet, P., Franck, F., Matagne, R.F., Remacle, C., 2006. ND3 and ND4L subunits of mitochondrial complex I, both nucleus encoded in Chlamydomonas reinhardtii, are required for activity and assembly of the enzyme. Eukaryot Cell 5, 1460-1467.
Cardol, P., Matagne, R.F., Remacle, C., 2002. Impact of mutations affecting ND mitochondria-encoded subunits on the activity and assembly of complex I in *Chlamydomonas*. Implication for the structural organization of the enzyme. J. Mol. Biol. 319, 1211-1221.
Cardol, P., Vanrobaeys, F., Devreese, B., Van Beeumen, J., Matagne, R., Remacle, C., 2004. Higher plant-like subunit composition of the mitochondrial complex I from *Chlamydomonas reinhardtii* : 31 conserved components among eukaryotes. Biochim. Biophys. Acta 1658, 212-224.
Carroll, J., Fearnley, I.M., Skehel, J.M., Shannon, R.J., Hirst, J., Walker, J.E., 2006. Bovine complex I is a complex of forty-five different subunits. J. Biol. Chem. 281, 32724-32727.
Debuchy, R., Purton, S., Rochaix, J.D., 1989. The argininosuccinate lyase gene of Chlamydomonas reinhardtii: an important tool for nuclear transformation and for correlating the genetic and molecular maps of the ARG7 locus. Embo J. 8, 2803-2809.
Dent, R.M., Haglund, C.M., Chin, B.L., Kobayashi, M.C., Niyogi, K.K., 2005. Functional genomics of eukaryotic photosynthesis using insertional mutagenesis of Chlamydomonas reinhardtii. Plant Physiol. 137, 545-556.
Duarte, M., Mota, N., Pinto, L., Videira, A., 1998. Inactivation of the gene coding for the 30.4-kDa subunit of respiratory chain NADH dehydrogenase: is the enzyme essential for Neurospora? Mol. Gen. Genet. 257, 368-375.
Emanuelsson, O., Nielsen, H., Brunak, S., von Heijne, G., 2000. Predicting subcellular localization of proteins based on their N-terminal amino acid sequence. J. Mol. Biol. 300, 1005-1016.
Erhardt, H., Steimle, S., Muders, V., Pohl, T., Walter, J., Friedrich, T., 2012. Disruption of individual nuo-genes leads to the formation of partially assembled NADH:ubiquinone oxidoreductase (complex I) in Escherichia coli. Biochim Biophys Acta 1817, 863-871.
Esterhazy, D., King, M.S., Yakovlev, G., Hirst, J., 2008. Production of reactive oxygen species by complex I (NADH:ubiquinone oxidoreductase) from Escherichia coli and comparison to the enzyme from mitochondria. Biochemistry 47, 3964-3971.
Ferrante, P., Ballottari, M., Bonente, G., Giuliano, G., Bassi, R., 2012. LHCBM1 and LHCBM2/7 polypeptides, components of major LHCII complex, have distinct functional roles in photosynthetic antenna system of Chlamydomonas reinhardtii. J Biol Chem 287, 16276-16288.

Fett, J.P., Coleman, J.R., 1994. Regulation of Periplasmic Carbonic Anhydrase Expression in Chlamydomonas reinhardtii by Acetate and pH. Plant Physiol 106, 103-108.
Friedrich, T., 2001. Complex I: a chimaera of a redox and conformation-driven proton pump? J. Bioenerg. Biomembr. 33, 169-177.
Glaser, E., Sjoling, S., Tanudji, M., Whelan, J., 1998. Mitochondrial protein import in plants. Plant Mol. Biol., 331-338.
González-Halphen, D., Funes, S., Perez-Martinez, X., Reyes-Prieto, A., Claros, M.G., Davidson, E., King, M.P., 2004. Genetic correction of mitochondrial diseases: using the natural migration of mitochondrial genes to the nucleus in chlorophyte algae as a model system. Ann. N.-Y. Acad. Sci. 1019, 232-239.
Gorman, D.S., Levine, R.P., 1965. Cytochrome f and plastocyanin: their sequence in the photosynthetic electron transport chain of *Chlamydomonas reinhardtii*. Proc. Natl. Acad. Sci. U. S. A. 54, 1665-1669.
Gray, M.W., Burger, G., Lang, B.F., 1999. Mitochondrial evolution. Science 283, 1476-1481.
Gutierres, S., Sabar, M., Lelandais, C., Chetrit, P., Diolez, P., Degand, H., Boutry, M., Vedel, F., de Kouchkovsky, Y., De Paepe, R., 1997. Lack of mitochondrial and nuclear-encoded subunits of complex I and alteration of the respiratory chain in *Nicotiana sylvestris* mitochondrial deletion mutants. Proc. Natl. Acad. Sci. U.S.A. 94, 3436-3441.
Hinchliffe, P., Sazanov, L.A., 2005. Organization of iron-sulfur clusters in respiratory complex I. Science 309, 771-774.
Jans, F., Mignolet, E., Houyoux, P.A., Cardol, P., Ghysels, B., Cuine, S., Cournac, L., Peltier, G., Remacle, C., Franck, F., 2008. A type II NAD(P)H dehydrogenase mediates light-independent plastoquinone reduction in the chloroplast of Chlamydomonas. Proc. Natl. Acad. Sci. U. S. A.
Kindle, K.L., 1990. High frequency nuclear transformation of *Chlamydomonas reinhardtii*. Proc. Natl. Acad. Sci. U. S. A. 87, 1228-1232.
Kobayashi, Y., Knoop, V., Fukuzawa, H., Brennicke, A., Ohyama, K., 1997. Interorganellar gene transfer in bryophytes: the functional nad7 gene is nuclear encoded in Marchantia polymorpha. Mol. Gen. Genet. 256, 589-592.
Kussmaul, L., Hirst, J., 2006. The mechanism of superoxide production by NADH:ubiquinone oxidoreductase (complex I) from bovine heart mitochondria. Proc Natl Acad Sci U S A 103, 7607-7612.
Lapaille, M., Thiry, M., Perez, E., Gonzalez-Halphen, D., Remacle, C., Cardol, P., 2010. Loss of mitochondrial ATP synthase subunit beta (Atp2) alters mitochondrial and chloroplastic function and morphology in Chlamydomonas. Biochim Biophys Acta 1797, 1533-1539.
Larosa, V., Coosemans, N., Motte, P., Bonnefoy, N., Remacle, C., 2012. Reconstruction of a human mitochondrial complex I mutation in the unicellular green alga Chlamydomonas. Plant J 70, 759-768.
Lecler, R., Vigeolas, H., Emonds-Alt, B., Cardol, P., Remacle, C., 2012. Characterization of an internal type-II NADH dehydrogenase from Chlamydomonas reinhardtii mitochondria. Curr Genet 58, 205-216.
Ledford, H.K., Chin, B.L., Niyogi, K.K., 2007. Acclimation to singlet oxygen stress in Chlamydomonas reinhardtii. Eukaryot Cell 6, 919-930.
Lelandais, C., Albert, B., Gutierres, S., De Paepe, R., Godelle, B., Vedel, F., Chetrit, P., 1998. Organization and expression of the mitochondrial genome in the Nicotiana sylvestris CMSII mutant. Genetics 150, 873-882.
Lemeille, S., Rochaix, J.D., 2010. State transitions at the crossroad of thylakoid signalling pathways. Photosynth. Res. .

Loppes, R., Radoux, M., 2001. Identification of short promoter regions involved in the transcriptional expression of the nitrate reductase gene in *Chlamydomonas reinhardtii*. Plant Mol. Biol. 45, 215-227.
Mathy, G., Cardol, P., Dinant, M., Blomme, A., Gerin, S., Cloes, M., Ghysels, B., DePauw, E., Leprince, P., Remacle, C., Sluse-Goffart, C., Franck, F., Matagne, R.F., Sluse, F.E., 2010. Proteomic and functional characterization of a Chlamydomonas reinhardtii mutant lacking the mitochondrial alternative oxidase 1. J Proteome Res 9, 2825-2838.
Merchant, S.S., Prochnik, S.E., Vallon, O., Harris, E.H., Karpowicz, S.J., Witman, G.B., Terry, A., Salamov, A., Fritz-Laylin, L.K., Marechal-Drouard, L., Marshall, W.F., Qu, L.H., Nelson, D.R., Sanderfoot, A.A., Spalding, M.H., Kapitonov, V.V., Ren, Q., Ferris, P., Lindquist, E., Shapiro, H., Lucas, S.M., Grimwood, J., Schmutz, J., Cardol, P., Cerutti, H., Chanfreau, G., Chen, C.L., Cognat, V., Croft, M.T., Dent, R., Dutcher, S., Fernandez, E., Fukuzawa, H., Gonzalez-Ballester, D., Gonzalez-Halphen, D., Hallmann, A., Hanikenne, M., Hippler, M., Inwood, W., Jabbari, K., Kalanon, M., Kuras, R., Lefebvre, P.A., Lemaire, S.D., Lobanov, A.V., Lohr, M., Manuell, A., Meier, I., Mets, L., Mittag, M., Mittelmeier, T., Moroney, J.V., Moseley, J., Napoli, C., Nedelcu, A.M., Niyogi, K., Novoselov, S.V., Paulsen, I.T., Pazour, G., Purton, S., Ral, J.P., Riano-Pachon, D.M., Riekhof, W., Rymarquis, L., Schroda, M., Stern, D., Umen, J., Willows, R., Wilson, N., Zimmer, S.L., Allmer, J., Balk, J., Bisova, K., Chen, C.J., Elias, M., Gendler, K., Hauser, C., Lamb, M.R., Ledford, H., Long, J.C., Minagawa, J., Page, M.D., Pan, J., Pootakham, W., Roje, S., Rose, A., Stahlberg, E., Terauchi, A.M., Yang, P., Ball, S., Bowler, C., Dieckmann, C.L., Gladyshev, V.N., Green, P., Jorgensen, R., Mayfield, S., Mueller-Roeber, B., Rajamani, S., Sayre, R.T., Brokstein, P., Dubchak, I., Goodstein, D., Hornick, L., Huang, Y.W., Jhaveri, J., Luo, Y., Martinez, D., Ngau, W.C., Otillar, B., Poliakov, A., Porter, A., Szajkowski, L., Werner, G., Zhou, K., Grigoriev, I.V., Rokhsar, D.S., Grossman, A.R., 2007. The Chlamydomonas genome reveals the evolution of key animal and plant functions. Science 318, 245-250.
Miura, K., Yamano, T., Yoshioka, S., Kohinata, T., Inoue, Y., Taniguchi, F., Asamizu, E., Nakamura, Y., Tabata, S., Yamato, K.T., Ohyama, K., Fukuzawa, H., 2004. Expression profiling-based identification of CO2-responsive genes regulated by CCM1 controlling a carbon-concentrating mechanism in Chlamydomonas reinhardtii. Plant Physiol 135, 1595-1607.
Noctor, G., De Paepe, R., Foyer, C.H., 2007. Mitochondrial redox biology and homeostasis in plants. Trends Plant Sci 12, 125-134.
Noguchi, K., Yoshida, K., 2008. Interaction between photosynthesis and respiration in illuminated leaves. Mitochondrion 8, 87-99.
Peters, K., Belt, K., Braun, H.P., 2013. 3D Gel Map of Arabidopsis Complex I. Front Plant Sci 4, 153.
Pineau, B., Mathieu, C., Gerard-Hirne, C., De Paepe, R., Chetrit, P., 2005. Targeting the NAD7 subunit to mitochondria restores a functional complex I and a wild type phenotype in the *Nicotiana sylvestris* CMS II mutant lacking nad7. J. Bio. Chem. 280, 25994-26001.
Pla, M., Mathieu, C., De Paepe, R., Chetrit, P., Vedel, F., 1995. Deletion of the last two exons of the mitochondrial nad7 gene results in lack of the NAD7 polypeptide in a Nicotiana sylvestris CMS mutant. Mol. Gen. Genet. 248, 79-88.
Ramachandran, G.N., Sasisekharan, V., 1968. Conformation of polypeptides and proteins. Adv Protein Chem 23, 283-438.
Remacle, C., Barbieri, M.R., Cardol, P., Hamel, P.P., 2008. Eukaryotic complex I: functional diversity and experimental systems to unravel the assembly process. Mol Genet Genomics 280, 93-110.

Remacle, C., Baurain, D., Cardol, P., Matagne, R.F., 2001. Mutants of *Chlamydomonas reinhardtii* Deficient in Mitochondrial Complex I. Characterization of two mutations affecting the nd1 coding sequence. Genetics 158, 1051-1060.
Remacle, C., Cardol, P., Coosemans, N., Gaisne, M., Bonnefoy, N., 2006. High-efficiency biolistic transformation of *Chlamydomonas* mitochondria can be used to insert mutations in complex I genes. Proc. Natl. Acad. Sci. U. S. A. 103, 4771-4776.
Remacle, C., Hamel, P., Larosa, V., Subrahmanian, N., Cardol, P., 2012. Chapter 11. Complexes I in the Green Lineage, in: Sazanov, L.A. (Ed.), A structural perspective on respiratory complex i. Springer, New York.
Rexroth, S., Meyer Zu Tittingdorf, J.M., Schwassmann, H.J., Krause, F., Seelert, H., Dencher, N.A., 2004. Dimeric H+-ATP synthase in the chloroplast of *Chlamydomonas reinhardtii*. Biochim. Biophys. Acta 1658, 202-211.
Saada, A., Vogel, R.O., Hoefs, S.J., van den Brand, M.A., Wessels, H.J., Willems, P.H., Venselaar, H., Shaag, A., Barghuti, F., Reish, O., Shohat, M., Huynen, M.A., Smeitink, J.A., van den Heuvel, L.P., Nijtmans, L.G., 2009. Mutations in NDUFAF3 (C3ORF60), encoding an NDUFAF4 (C6ORF66)-interacting complex I assembly protein, cause fatal neonatal mitochondrial disease. Am J Hum Genet 84, 718-727.
Sazanov, L.A., Hinchliffe, P., 2006. Structure of the hydrophilic domain of respiratory complex I from Thermus thermophilus. Science 311, 1430-1436.
Sazanov, L.A., Peak-Chew, S.Y., Fearnley, I.M., Walker, J.E., 2000. Resolution of the membrane domain of bovine complex I into subcomplexes: implications for the structural organization of the enzyme. Biochemistry 39, 7229-7235.
Schroda, M., 2006. RNA silencing in *Chlamydomonas*: mechanisms and tools. Curr. Genet. 49, 69-84.
Schulte, U., Weiss, H., 1995. Generation and characterization of NADH: ubiquinone oxidoreductase mutants in Neurospora crassa. Methods Enzymol. 260, 3-14.
Silflow, C.D., 1998. Organization of the Nuclear Genome, in: Rochaix, J.D., Goldschmidt-Clermont, M., Merchant, S. (Eds.), The molecular biology of choloroplasts and mitochondria in Chlamydomonas. Kluwer Academic Publishers, pp. 25-40.
Takahashi, H., Iwai, M., Takahashi, Y., Minagawa, J., 2006. Identification of the mobile light-harvesting complex II polypeptides for state transitions in Chlamydomonas reinhardtii. Proc. Natl. Acad. Sci. U. S. A. 103, 477-482.
Tardif, M., Atteia, A., Specht, M., Cogne, G., Rolland, N., Brugiere, S., Hippler, M., Ferro, M., Bruley, C., Peltier, G., Vallon, O., Cournac, L., 2012. PredAlgo: a new subcellular localization prediction tool dedicated to green algae. Mol Biol Evol 29, 3625-3639.
Villavicencio-Queijeiro, A., Vazquez-Acevedo, M., Cano-Estrada, A., Zarco-Zavala, M., Tuena de Gomez, M., Mignaco, J.A., Freire, M.M., Scofano, H.M., Foguel, D., Cardol, P., Remacle, C., Gonzalez-Halphen, D., 2009. The fully-active and structurally-stable form of the mitochondrial ATP synthase of Polytomella sp. is dimeric. J. Bioenerg. Biomembr. 41, 1-13.
Vogel, R.O., Smeitink, J.A., Nijtmans, L.G., 2007. Human mitochondrial complex I assembly: A dynamic and versatile process. Biochim Biophys Acta 1767, 1215-1227.

Figure 1

Click here to download high resolution image

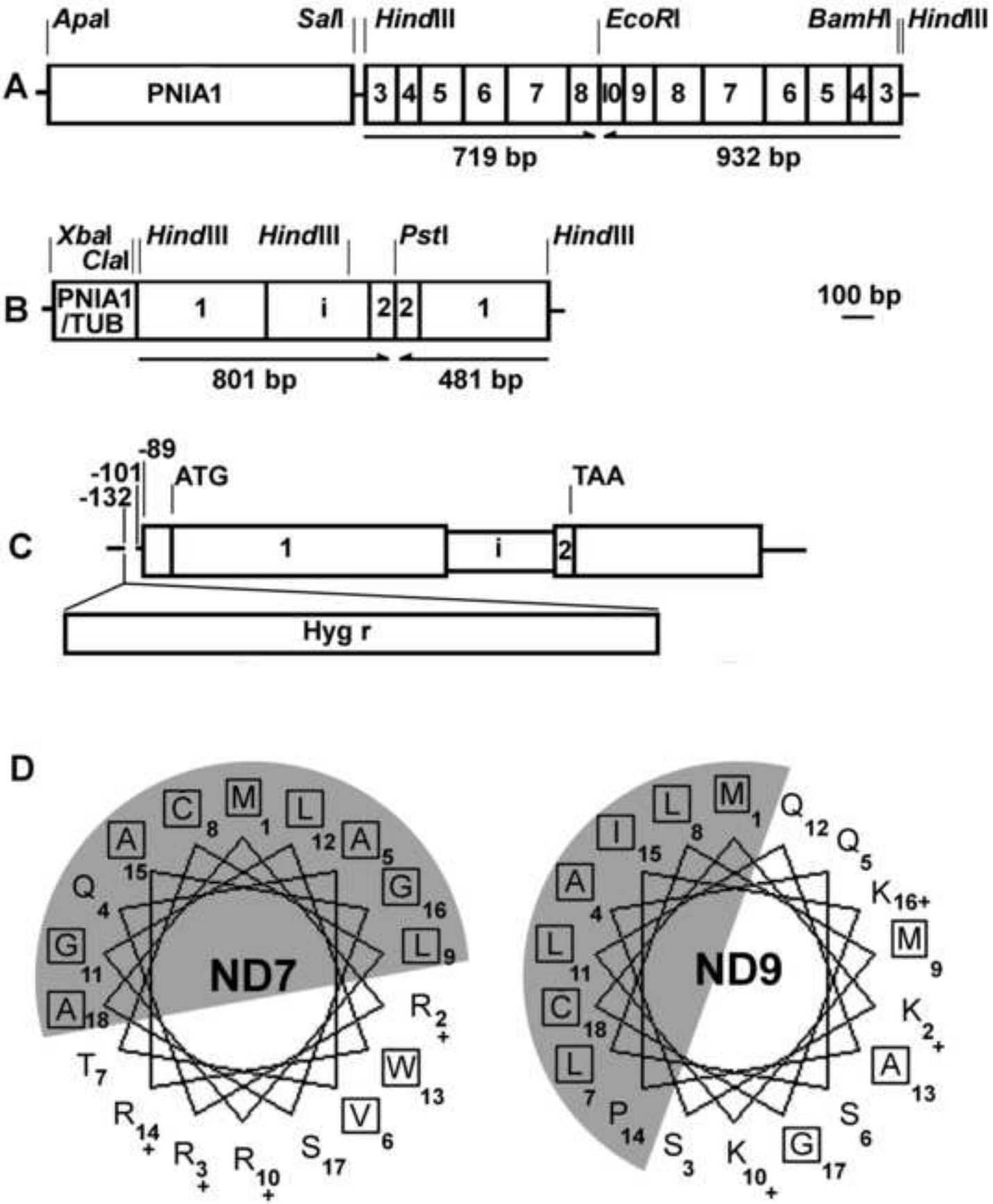

Figure 2

Click here to download high resolution image

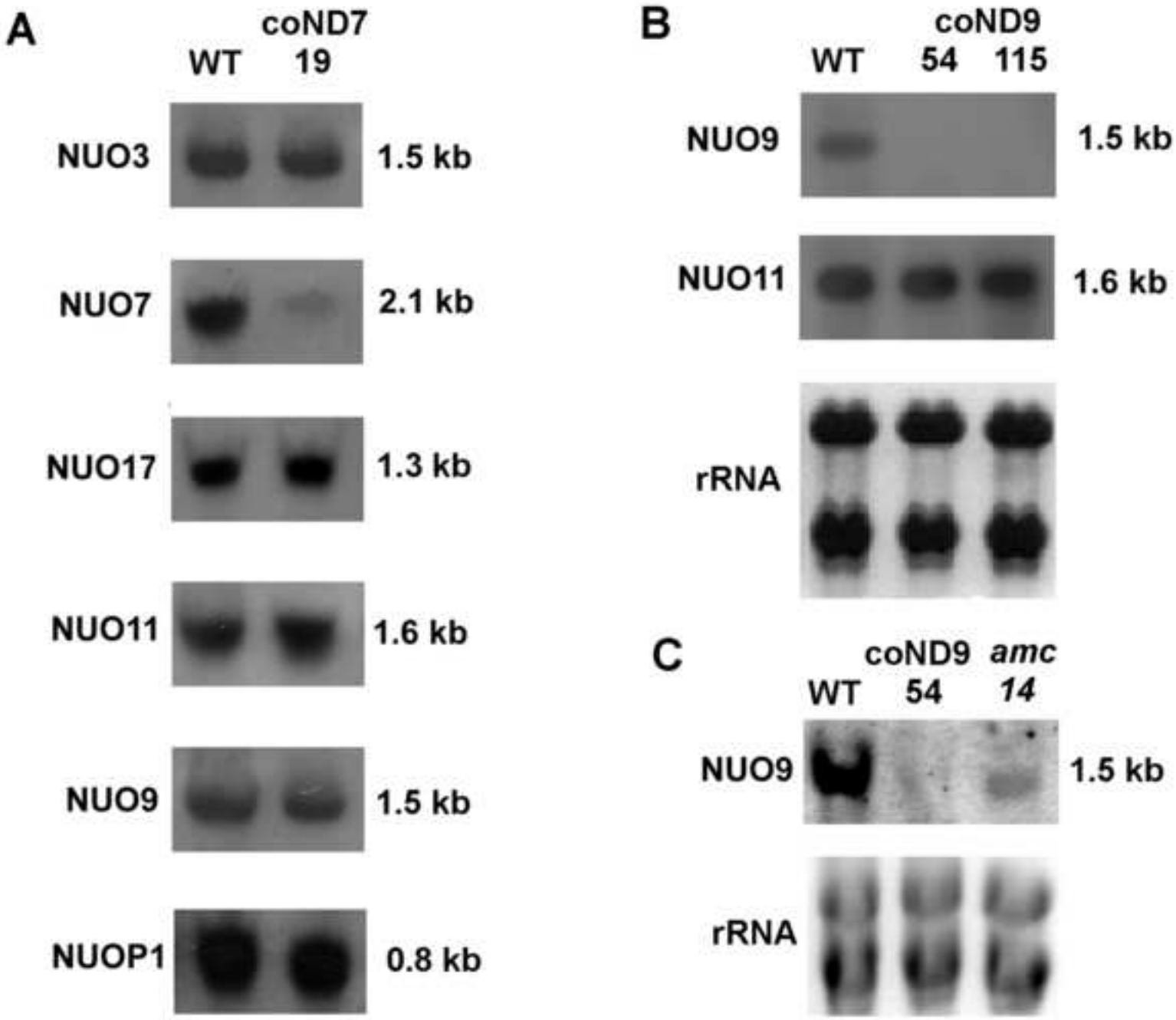

Figure 3

Click here to download high resolution image

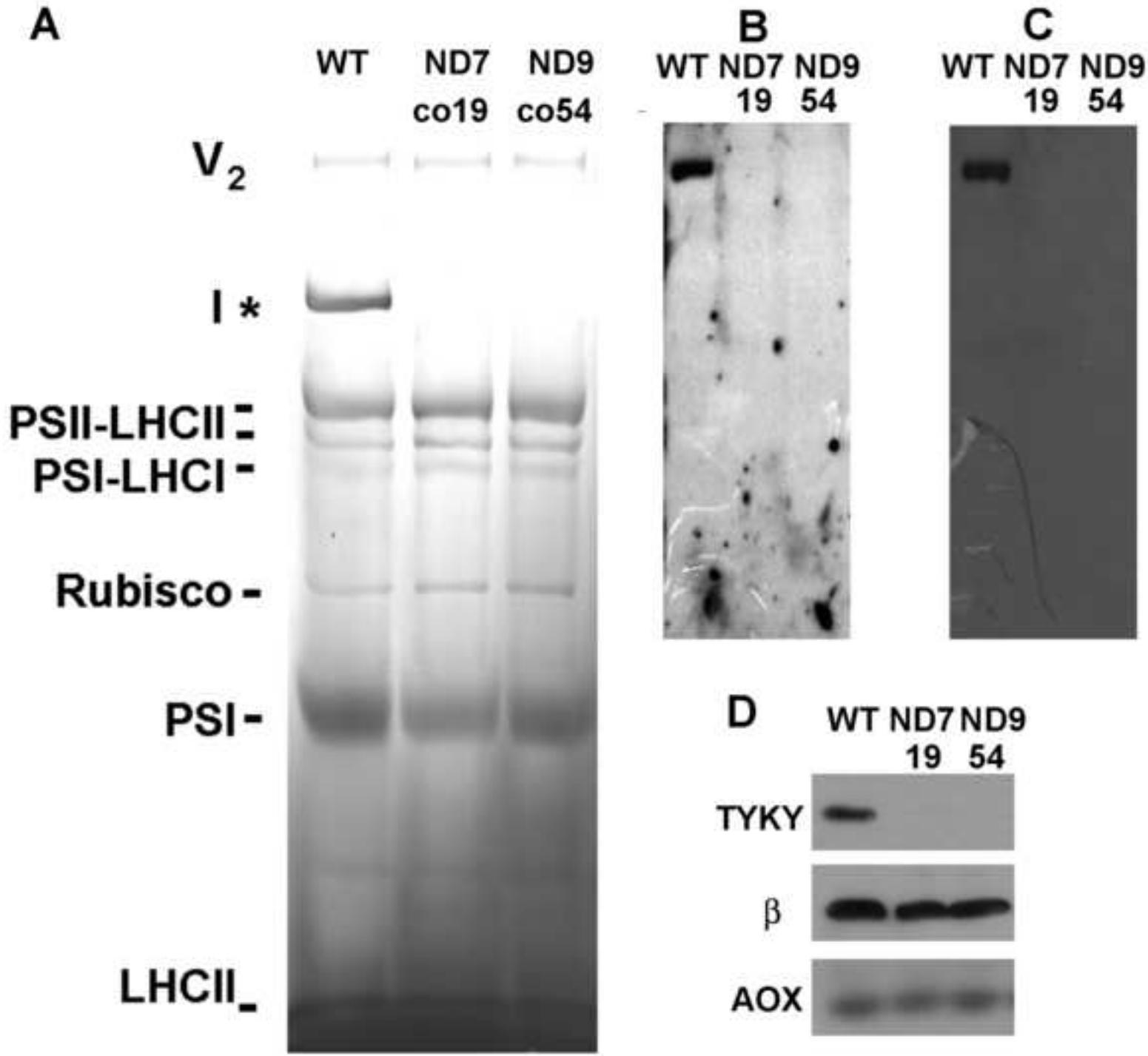

Table 1 revised

	Control WT	Nd7 co-19	Nd9 co-54	Nd9 co-115	Nd9 *amc14*	ND6 *dum17*
Total respiration	41 ± 3	26 ± 2	28 ± 4	nd	26 ± 3	20 ± 4
Rotenone-sensitive respiration	26 ± 3	2 ± 1	2 ± 2	nd	11 ± 2	3 ± 3
NADH:DQ oxidoreductase [a]	108 ± 21	43 ± 6	50 ± 12	45 ± 8	78 ± 12	61 ± 13
Complex I activity[b]	53 ± 13	1.4 ± 0.8	2.1 ± 1.5	1.2 ± 1.1	27 ± 10	0
NADH:$Fe(CN)_6^{3-}$ oxidoreductase [c]	2312 ± 424	786 ± 222	401 ± 113	289 ± 57	1346 ± 189	389 ± 86
Complex IV activity [d]	237 ± 18	218 ± 4	263 ± 23	202 ± 24	262 ± 44	182 ± 51

Table 1. Respiratory rates (nmol O_2 . min^{-1} . 10^{-7} cells) of wild-type and mutant cells were measured in the absence or in the presence of 100 μM rotenone. Specific enzyme activities were measured in crude membrane fractions: [a]NADH:duroquinone oxidoreductase (nmoles of NADH oxidized . min^{-1} . mg $protein^{-1}$); [b]Rotenone-sensitive NADH:duroquinone oxidoreductase (nmoles of NADH oxidized . min^{-1} . mg $protein^{-1}$); [c]NADH:ferricyanide oxidoreductase (nmoles of $K_3Fe(CN)_6^{3-}$ reduced . min^{-1} . mg $protein^{-1}$); [d]Cytochrome *c* oxidase (nmoles of cytochrome *c* oxidized . min^{-1} . mg $protein^{-1}$). nd, not determined. Means ± SD from three to six experiments.

Table 2

	WT	*dum17*	coND7-RNAi	coND9-RNAi
Chlorophyll $_{a+b}$	1 ± 0.04	0.95 ± 0.06	1.01 ± 0.03	0.98 ± 0.02
PSII antenna size	1 ± 0.12	1.14 ± 0.08	0.96 ± 0.08	0.92 ± 0.09
Pmax	1 ± 0.22	0.89 ± 0.12	0.85 ± 0.23	0.90 ± 0.21
H_2O_2	1 ± 0.07	0.65 ± 0.06	0.75 ± 0.31	0.88 ± 0.22

Table 2. Photosynthetic parameters and hydrogen peroxide production of complex I-deficient mutant cells relative to wild-type cells in mixotrophic conditions (light + acetate). Chlorophyll$_{a+b}$ (23.8 ± 0.8 µg per 10^7 cells for wild-type cells). PSII antenna size were estimated as t½ (s) of chlorophyll fluorescence induction kinetics in the presence of DCMU at low light. Pmax, maximum rate of oxygen evolution in saturating light (61 ± 14 nmoles O_2 . min^{-1} per 10^7 cells in WT). Hydrogen peroxide production (DAB staining, arbitrary unit). Average of WT $mt^{+/-}$ $cw^{+/-}$ strains and complex I deficient mutants (233 and 680 *dum17* strains; coND7 and coND9 strains) incubated in white light (50 µE m^{-2} s^{-1}). Mean value obtained for control cells were arbitrarily fixed to 1 (mean ± SD of >3 experiments).

Table 3

Gene	Name	#spots (average ratios (CI-/WT)	Protein ID
	Mitochondrial respiratory chain		
NUO9	Complex I Nd9 subunit	1 (-2.1*)	gi|159464845
NUOA9	Complex I 39 kDa subunit	1 (-1.9*)	gi|159489336
QCR1	Complex III 50kD core 1 subunit	1 (-1.1)	gi|159477849
ATP1A	F1F0 ATP synthase alpha subunit	1 (1)	gi|159483185
ATP2	F1F0 ATP synthase beta subunit	2 (1,-1.1)	gi|159466892
ASA7	F1F0 ATP synthase Asa7 subunit	1 (1)	gi|159477303
	ROS scavenging		
FSD1	chloroplastic superoxide dismutase [Fe]	1 (-1.5*)	gi|159464723
GSTS2	glutathione S-transferase	1 (-1.7*)	gi|159482414
MSD1/SODA	mitochondrial superoxide dismutase [Mn]	1 (-1.6*)	gi|159484019
	Krebs cycle, Glycolysis, Glyoxylate cycle		
AST1	mitochondrial aspartate aminotransferase	1 (+2.0*)	gi|159473837
AST3	chloroplastic aspartate aminotransferase	1 (+1.3*)	gi|159483981
PGK1	phosphoglycerate kinase	1 (+1.1)	gi|159482940
ICL	isocitrate lyase	5 (-1.1,-1.1,-1.1,1,+1.3)	gi|619932
MAS	malate synthase	2 (-1.2,-1.1)	gi|159475042
ACH1	aconitate hydratase	7(+1.1,+1.1,+1.1,+1.1,+1.3,1.4,+1.4*)	gi|159462944
ACS3	acetyl CoA synthetase	1 (1)	gi|159488061
IDH3	NADP-dependent isocitrate dehydrogenase	1 (+1.1)	gi|159481269
GCSL	dihydrolipoyl dehydrogenase	1 (+1.3)	gi|159474092
	Photosynthesis, Calvin cycle, Carbon fixation		
CAH1	periplasmic carbonic anhydrase alpha	3 (-2.4*,-2.8*,-6.7*)	gi|159468241
CA1	mitochondrial carbonic anhydrase beta	2 (-1.2, -1.8)	gi|1323549
OEE1	oxygen-evolving enhancer protein 1	3 (-1.1,-1.1,-1.1)	gi|74272687
OEE2	oxygen-evolving enhancer protein 2	2 (-1.1,-1.9)	gi|159471964
LHCB M1	light-harvesting complex II protein	1 (1)	gi|20269804
LHCB M2	light harvesting complex II protein	2 (-1.2, -1.5*)	gi|4139216
LHCB M3	light harvesting complex II protein	3 (-1.3,1,+1.2)	gi|159491492
LHCB5	light harvesting complex II protein	1 (-1.5*)	gi|159475641
LHCB M10	light harvesting complex II protein	4 (-1.1,-1.2,-1.2,-1.2)	gi|19423285
ATPA	ATP synthase CF1 alpha subunit	2 (+1.1,+1.2)	gi|1334356
ATPB	ATP synthase CF1 beta subunit	3 (+1.1,+1.1,+1.4)	gi|41179057
ATPC	ATP synthase CF1 gamma subunit	1 (-1.3)	gi|159476472
GAP1b	glyceraldehyde-3-phosphate dehydrogenase	3 (1, -1.2,-1.3)	gi|159490469
PRK1	phosphoribulokinase	1 (+1.3)	gi|159471788
RBCL	Rubisco large subunit	13 (-1.1,-1.1,1,1,1,1,+1.1,+1.1,+1.1,+1.2,+1.3,+1.3,+1.4)	gi|5360587
RBCS	Rubisco small subunit	1 (-3.7*)	gi|16975084
RCA1	Rubisco activase	2 (-1.1,1)	gi|159468147

SEBP1	sedoheptulose-1; 7-bisphosphatase	2 (1,+1.3)	gi|159467635
TAL1	transaldolase	1 (+1.1)	gi|159463680
TRK1	transketolase	4 (-1.2,-1.3,-1.4,-1.5)	gi|159487741
STA6	ADP-glucose pyrophosphorylase small subunit	1 (+1.1)	gi|159467349
	Chlorophyll biosynthesis		
DXR1	1-deoxy-D-xylulose 5-phosphate reductoisomerase	1 (+1.2)	gi|159471628
ChlH	magnesium chelatase subunit I	2 (+1.1,+1.2)	gi|159466070
ChlP	geranylgeranyl reductase	1 (1)	gi|159464036
POR	light-dependent protochlorophyllide reductase	1 (-1.2)	gi|159462468
PPX1	protoporphyrinogen oxidase	1 (+1.4)	gi|159472731

Table 3. Effects of complex I loss on soluble proteins involved energetic metabolism. Number of spots identified for each proteins are given with the average ratio (see Table S2 for details). *, t-test $p < 0.05$.

Figure S1

Click here to download Supplementary material: FIGURE_S1_Massoz.rtf

Figure S2

Click here to download Supplementary material: FIGURE_S2_Massoz.tif

Figure S3

Click here to download Supplementary material: FIGURE_S3_massoz.pptx

Table S1

Click here to download Supplementary material: TABLE_S1_MASSOZ.doc

Table S2

Click here to download Supplementary material: TABLE_S2_MASSOZ.doc